Quantitative relation between structure and thermal conductivity in type-I clathrates $X_8Ga_{16}Ge_{30}$ (X = Sr, Ba) based on electrostatic-potential analysis

Akihiko Fujiwara,[1,2,*] Kunihisa Sugimoto,[1,3] Che-Hsiu Shih,[3,4] Hiroshi Tanaka,[5] Jun Tang,[6] Yoichi Tanabe,[6] Jingtao Xu,[6] Satoshi Heguri,[2] Katsumi Tanigaki,[2,6] and Masaki Takata[1,3,4]

[1]*Japan Synchrotron Radiation Research Institute (JASRI), SPring-8, Hyogo 679-5198, Japan*
[2]*Department of Physics, Tohoku University, Sendai 980-8578, Japan*
[3]*RIKEN SPring-8 Center, Hyogo 679-5148, Japan*
[4]*Department of Advanced Materials, University of Tokyo, Chiba 277-8561, Japan*
[5]*Department of Materials Science, Shimane University, Shimane 690-8504, Japan*
[6]*WPI Advanced Institute for Materials Research, Tohoku University, Sendai 980-8578, Japan*

(Received 10 January 2012; published 17 April 2012)

In order to quantitatively characterize the effect of motion of the guest atom in type-I clathrates $X_8Ga_{16}Ge_{30}$ (X = Sr, Ba) on thermal conductivity, electrostatic potential in the crystal was visualized by synchrotron radiation x-ray diffraction. The obtained electrostatic potential clearly exhibited structural aspects of the guest atom, rattling, which is considered as a cause of suppression of thermal conductivity κ. The parameterized degree of rattling "rattling factor," f_R, being defined as a volume ratio of the electrostatic interaction region of the guest atom to the spherical volume estimated by the covalent radius of the guest atom, was found to well classify κ. The κ monotonously decreases with increasing the f_R. Consequently, f_R was judged as a better criterion to explore high-performance thermoelectric system of the clathrates.

DOI: 10.1103/PhysRevB.85.144305 PACS number(s): 82.75.−z, 61.05.cp, 72.20.Pa

I. INTRODUCTION

Of particular interest is a peculiar motion of guest atoms, ions and clusters confined in nanospace, which provides unexplored physical and chemical properties, such as magnetic,[1] dielectric,[2] and superconducting,[3] characteristics and selective gas sorption.[4] An anomalous motion of the guest atoms inside the cage-structured host lattice, so-called "rattling," is one of the prominent examples of an origin of unconventional thermoelectric (skutterudites[5–8] and clathrates[9,10]) and superconducting (pyrochlore[11,12]) properties. As for the thermoelectric properties, it has been suggested that the rattling suppresses thermal conductivity, κ, through phonon scattering without significant reduction of electrical conductivity, σ. The behavior interpreted as "phonon glass and electron crystal" state[13,14] fascinates many researchers in both fundamental and applied science, because it can be applicable to practical (high-performance) thermoelectric devices. The figure of merit of thermoelectric materials $Z = S^2\sigma/\kappa$ becomes higher for the higher Seebeck coefficient, S, higher σ, and lower κ. Because these parameters are not independent (σ and κ tend to show similar trends), the tradeoff between enhancement and reduction in σ and κ is always one of the gravest obstacles for improving efficiency. Consequently, the use of rattling has been considered to be a decisive approach for thermoelectric applications. On the other hand, Koza *et al.* found that the rattling is coherently coupled with the host-lattice dynamics, and it cannot result in "phonon glass" in skutterudites.[7] Therefore, the nature of rattling in the host-guest systems still remains to be unveiled.

Recently, it has been reported that the type-I clathrate compounds, $X_8Ga_{16}Ge_{30}$ (X = Sr, Ba, Eu), show wide variety of electrical and thermal properties, although differences of their crystal structure are quite small.[15,16] Generally expected values of κ were observed in n-type $Ba_8Ga_{16}Ge_{30}$ (n-BGG), whereas the values of κ for both p-type $Ba_8Ga_{16}Ge_{30}$ (p-BGG) and n-type $Sr_8Ga_{16}Ge_{30}$ (n-SGG) were suppressed and showed small temperature dependence.[17–22] On the other hand, the crystal structure of these compounds has the same lattice framework (cubic structure with the space group of $Pm\bar{3}n$) consisting of $(Ga/Ge)_{20}$ and $(Ga/Ge)_{24}$ polyhedron cages with a guest atom of X in each cage.[15,16,23] For understanding their characteristics, experiments on thermal properties,[17–22] acoustic properties,[24] neutron scattering,[25] Raman scattering,[26–28] optical conductivity,[29–31] extended x-ray fine-structure analysis,[32] and soft x-ray spectroscopy[33] as well as theoretical modeling[34–38] have been intensively performed. These results suggested that glasslike low κ observed in crystalline materials originating from the rattling, which is the off-center distribution of the guest $X(2)$ atom inside the $(Ga/Ge)_{24}$ polyhedron (Fig. 1), and this behavior was significant at low temperatures.[8,23] Although these compounds are suitable for further insight into the nature of rattling based on intensive studies,[9,10,13–38] the quantitative relation between the degree of motion and the κ values has not been clarified. As the rattling is dominated by the weak electrostatic interaction between the host cage and guest atom,[29,34–38] electron charge distributions and the resulting electrostatic potential around the guest $X(2)$ atom interaction should include valuable information. In this paper, we visualize the electrostatic potential influenced by rattling, based on a sequential analysis of electron density and electrostatic potential, using synchrotron radiation x-ray diffraction data at 20 K for single crystals of n-BGG, p-BGG, and n-SGG. In addition, we show that the value quantified from our electrostatic-potential analysis is a good criterion for the reduction of κ.

II. EXPERIMENTAL

Single-crystalline samples of $X_8Ga_{16}Ge_{30}$ (X = Sr, Ba) were grown using a self-flux method from stoichiometric

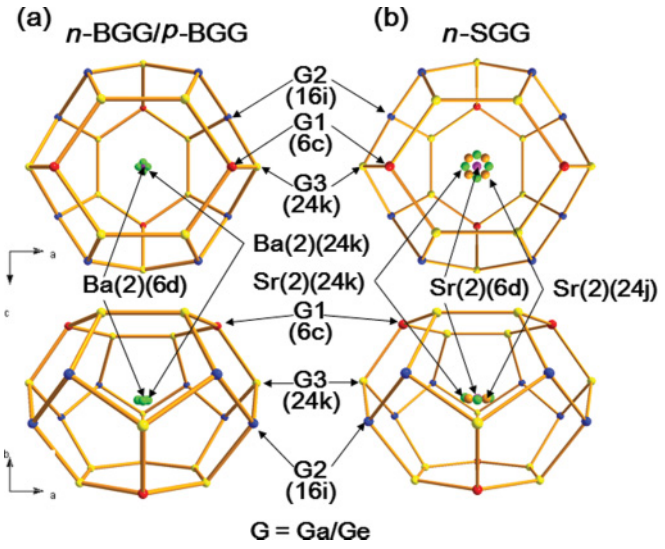

FIG. 1. (Color online) Structure of $(Ga/Ge)_{24}$ cage and $X(2)$ guest, $X(2)$ $(Ga/Ge)_{24}$. (a) n-BGG and p-BGG. (b) n-SGG.

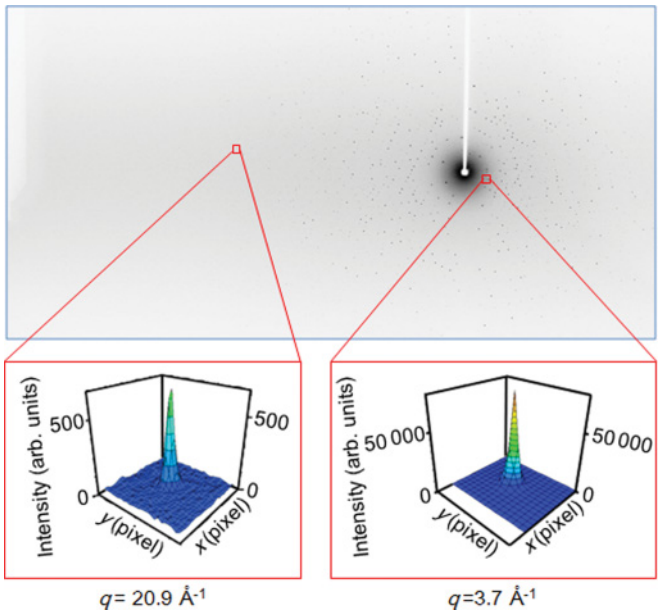

FIG. 2. (Color online) Typical diffraction image and examples of diffraction profile for p-BGG.

amounts of Ba, Sr, and Ge under an excessive amount of Ga, and control of p- and n-type semiconducting character in $Ba_8Ga_{16}Ge_{30}$ was achieved by tuning the Ba/Ga ratio.[19–22,33] The samples were characterized using inductively coupled plasma (ICP) analyses.

Synchrotron radiation (SR) x-ray diffraction measurements were carried out at BL02B1, SPring-8, Japan. SR x rays from a bending magnet were monochromatized to an energy of 34.92 keV ($\lambda = 0.355$ Å) by a monochromator with a double-crystal Si(111). The beam was focused by a sagittal-focusing monochromator and a bent mirror made of Si crystal coated with Pt. The focused beam size at the sample position was about 0.3×0.3 mm^2. The number of photons was about 10^{10} photon/s at the sample position. A cylindrical imaging plate with the camera length of 191.3 mm was adopted. Each side of the single crystal was less than 20 μm. Nine frames of diffraction images in the scattering vector (q) range up to about 34 Å^{-1} were taken with an exposure time of 63, 42, and 37 min for n-BGG, p-BGG, and n-SGG, respectively. All measurements were performed at 20 K (lowest temperature in the system) by cryogenic He flowing system (XR-HR10K-S, Japan Thermal Engineering Co. Ltd.), because the rattling is significant relative to the normal thermal vibrations at low temperature: a stationary off-center distribution in the clathrates would particularly influence the thermal conductivity at low temperatures.[8,23] The oscillation angle of the crystal (ω) in each frame was 10°. A typical example of diffraction image and profiles for p-BGG are shown in Fig. 2.

Precise structural analysis was performed with the sequence of the atom-coordination determination using Fourier maps, the electron density distribution analysis by a maximum entropy method (MEM) and the electrostatic-potential analysis. For unveiling the effect of the subtle structural difference among three kinds of compounds, experimental and analysis conditions, including the data set, were strictly unified, which is one of the advantages to the pioneer MEM studies.[39,40] Reflections used for analysis were selected so that the same reflections are adopted for three compounds and the completeness becomes 100%. In this condition, the number of reflections was 1206 in the q-range from 0.5 Å^{-1} to 13.7 Å^{-1}.

All structures were solved by direct methods (SHELXS-97) and refined by full-matrix least squares techniques on F^2 (SHELXL-97). We used anomalous dispersion coefficients for structure refinement, f' and f'', in dependence on x-ray energy calculated on the original FPRIME code of Cromer,[41] which are $f' = -2.18732$ and $f'' = 0.65824$ for barium, $f' = 0.226773$ and $f'' = 0.45771$ for gallium, and $f' = 0.23860$ and $f'' = 0.51770$ for germanium. Because of small size of the samples, it was not necessary to carry out absorption and extinction correction for the high energy x-ray beam with the energy of about 35 keV. For all compounds, no attempt was made to distinguish between Ga and Ge for the three cage sites of 6c (denoted G1), 16i (denoted G2), and 24k (denoted G3; Fig. 1), because the difference between electron densities of Ga and Ge in the clathrate is too small to be distinguished by x-ray diffraction. On the other hand, the total electron number may influence the following MEM analysis so that we focused on the accurate estimation of total electron number of each site using the average ratio of Ga and Ge with introducing defects. Further details of the crystal structure investigations can be obtained from the Fachinformationszentrum Karlsruhe on quoting the depository number CSD-422586,[42] CSD-422587[43] and CSD-422585,[44] for n-BGG, p-BGG, and n-SGG, respectively. Diamond software (Crystal Impact) and OpenDX were used for graphical representation.

Electron density distribution was analyzed by the MEM[45,46] with the unit cell divided into $256 \times 256 \times 256$ pixels: a unit is a cubic with one side about 0.042 Å in length. The electrostatic potential $U(r)$ is obtained by the sum of electron and nucleus charge components, $U_{ele}(r)$ and $U_{nuc}(r)$, respectively.[47,48] The $U_{ele}(r)$ is sensitive to the electron-charge-density distribution, so it was directly calculated from the MEM charge density in the reciprocal space. On the other hand, the $U_{nuc}(r)$ is estimated by the ordinary Ewald's method using the atomic positions

TABLE I. List of occupancy of sites in X(2)(Ga/Ge)$_{24}$ cage for n-BGG, p-BGG, and n-SGG based on conventional structure analysis.

	Occupancy of host site			Occupancy of guest site		
	G1 (6c)	G2 (16i)	G3 (24k)	On-center (6d)	Off-center (24k)	Off-center (24j)
n-BGG	0.9991(1)	1.004(8)	0.9971(7)	1.0	–	–
p-BGG	0.985(2)	0.999(2)	0.995(2)	0.3315(8)	0.1684(5)	–
n-SGG	0.9917(9)	1.007(7)	1.001(7)	0.020(4)	0.0778(9)	0.1688(6)

taking account of anisotropic thermal displacement estimated by the conventional analysis.

III. RESULTS AND DISCUSSION

A. Fundamental structures

Fundamental crystal structures of three kinds of compounds[42–44] determined by the conventional structural analysis based on the Fourier method are consistent with those of previous reports.[15,16,23] No significant difference was observed among three kinds of compounds except for the defect in a cage-structured host site and the position of the guest atom $X(2)$ (Table I). A small but unnegligible amount [1.5(2)%] of defects was found only in the G1 site of p-BGG. In accordance with the subtle change in cage structure, more than 65% of guest Ba(2) atoms in the (Ga/Ge)$_{24}$ cages are distributed to the off-center site (24k), and only about 33% of guest Ba(2) atoms remain at the on-center site (6d) for p-BGG. Four equivalent 24k sites of the guest atom do not lie on a plane but forms a saddlelike shape as to compensate the lack of electron at the G1 site. The change (reduction) of electron number of p-BGG from n-BGG due to the defects was estimated as 7.28 per chemical formula and is consistent with the change of the carrier type from electron (n-type) to hole (p-type).[17–22,26–28] Although the value is a few times larger than that of previous reports,[19–22] we confirmed the small overestimation in comparison with the total electron number (about 1900 electrons per chemical formula) hardly affect our conclusion. On the other hand, no clear difference in cage structure was observed between n-BGG and n-SGG. Even though the cage structure of n-SGG is almost the same as that of n-BGG, the guest Sr(2) atoms are widely distributed to 24k and 24j sites, and only 2% of Sr(2) atoms remain at the on-center site (6d). This can be attributed to a smaller ionic radius of Sr.

B. Electron density distribution

We further carried out electron density analysis by the MEM.[45,46] Figure 3(a) shows the isosurface of electron density with a value of 1.5 electron/Å^3 (e/Å^3) for the fundamental cage components consisting the crystal structure, i.e., $X(1)$(Ga/Ge)$_{20}$ and $X(2)$(Ga/Ge)$_{24}$ cages. Reliable factors of MEM analysis (R_{MEM}) were 3.52, 1.55, and 2.16% for n-BGG, p-BGG, and n-SGG, respectively. The MEM electron density distributions of the guest atom for three compounds are different according to the different disordered positions and/or thermal vibrations of the guest atoms. From the results, it is suggested that a guest $X(2)$ atom tends to spread around the on-center site even in n-BGG, and the displacement and/or degree of distribution are enhanced in p-BGG and n-SGG. By conventional analysis discussed in the Sec. III A, the wide electron distribution of n-BGG was simply attributed to the symmetric on-center site (6d) using huge atomic displacement parameters (ADPs), $U_{22} = U_{33} = 24.38(8) \times 10^{-3}$ Å^2,[42] because the displacement of the guest atom $X(2)$ from the on-center position is not enough large to be distinguished by the conventional structural analysis. When the displacement becomes larger in p-BGG and n-SGG, on the other hand, an existence of additional off-center atomic positions (24k and 24j) were required with reasonable ADPs, $U_{22} = U_{33} < 1.8 \times 10^{-3}$ Å^2.[43,44] Because the MEM is a method of the electron density refinement best fitted to the observed diffraction data, the MEM can faithfully represent the subtle features of electron density at the interatomic region such as the bonding nature as well as the charge concentration at the atomic site beyond the structural model.[2,45,46,49–51] It should be noted that we confirmed that the slight difference in the structural model

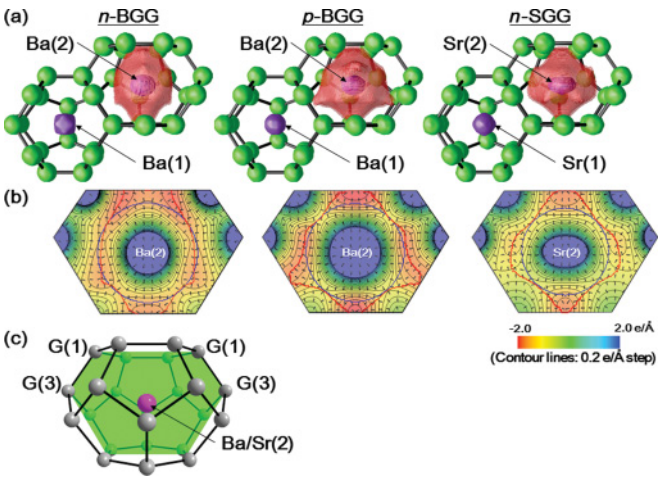

FIG. 3. (Color online) Structural characterization by the charge-density analysis using MEM and following the electrostatic-potential analysis. (a) Perspective view of electron density isosurface with a value of 1.5 e/Å^3 for $X(1)$(Ga/Ge)$_{20}$ and $X(2)$(Ga/Ge)$_{24}$ cages [green (medium gray) and purple (dark gray)]. Surface in puce surrounding the X(2) atom represents the trace of local minimum in electrostatic potential in the $X(2)$(Ga/Ge)$_{24}$ cage. (b) Cross sections of electrostatic-potential maps in X(2)(Ga/Ge)$_{24}$ cage with the range between −2.0 and 2.0 e/Å. Cross sections are vertical sections, including the two G1 cite at the top side and the center of $X(2)$(Ga/Ge)$_{24}$ cage as shown in (c) by a green plane. Arrows in (b) show the direction of electric field at each point. Red curves and blue circles correspond to the trace of the local minimum point of the electrostatic potential and the circle with the covalent radius of the atom, respectively.

TABLE II. Physical parameters of guest atoms, cages, and rattling factor.

	Number of electrons inside the EPLMS[a]	Volume inside the EPLMS V_{EP} (Å^3)[b]	Size of the guest atom V_{cov} (Å^3)[c]	Size of the cage V_{cage} (Å^3)[d]	Rattling factor $f_R \equiv V_{EP}/V_{cov}$
n-BGG	55.646(3)	37.48(1)	41.630	303.42	0.90005(3)
p-BGG	55.727(2)	47.092(9)	41.630	302.99	1.1312(2)
n-SGG	38.0474(1)	37.952(1)	31.059	298.84	1.22193(4)

[a]Estimated by integrating electron charge density in the area surrounded by the EPLMS depicted in Fig. 3(a).
[b]Defined as a volume of the area surrounded by the EPLMS depicted in Fig. 3(a).
[c]Defined as a volume of atomic sphere using the covalent radius r_{cov},[52] $V_{cov} \equiv 4\pi r_{cov}^3/3$.
[d]Defined as a volume of cage using atomic coordination obtained by conventional structural analysis.

among the three compounds obtained by the refinement does not bias the resulting MEM charge densities in the present study on the analysis of the single-crystalline samples.

C. Electrostatic-potential distribution

The rattling of the guest atom should influence the charge-density distribution and then the resulting electrostatic potential around the guest atom. Thus, it is meaningful to visualize electrostatic potential inside the $(Ga/Ge)_{24}$ cage. We applied a method to transform the MEM electron density into electrostatic potential to examine the interatomic interaction inside the cage.[47,48] Figure 3(b) shows cross sections [green area of Fig. 3(c)] of electrostatic potential in the $X(2)(Ga/Ge)_{24}$ cages of *n*-BGG, *p*-BGG, and *n*-SGG. The red curves represent grooves of the electrostatic potential between the guest atom, $X(2)$, and the cage, $(Ga/Ge)_{24}$. The three-dimensional representation of this boundary surface, namely, electrostatic-potential local-minimum surfaces (EPLMS) are inserted in Fig. 3(a) in puce. A difference in directional feature of the EPLMS among the three compounds is more obvious than the subtle difference in the isosurface of MEM charge density in Fig. 3(a). In Fig. 3(b), electric fields derived from the electrostatic potential are indicated by arrows and are found to be directed from the guest atom, $X(2)$, to the EPLMS. This means that EPLMS is the electrostatic interaction-free surface. Thus, the number of electrons inside the EPLMS ought to be the total electron number of the neutral atom in the EPLMS regardless of the valence of the guest atom, ionic or neutral. In fact, the values calculated from the MEM charge density for three compounds (Table II) are in good accordance with those of the corresponding guest atoms, 56 for Ba and 38 for Sr. The fractional difference from the exact number may be due to the accuracy of the number estimation from grid data of charge-density distribution. It should be noted that redistribution of electron charge, such as charge transfer from and to the guest atoms, causes the enlargement and shrinkage of the regions surrounded by the EPLMS, respectively. Therefore, the region inside the EPLMS should correspond to that electrostatically influenced by the atom/ion in the EPLMS, i.e., electrostatic interaction region by the guest atom.

The factor to change the electrostatic interaction region is the valence change and/or the displacement of the guest atoms. Because the nominal valence of the guest atoms for the three compounds is the same, the difference in size of the electrostatic interaction region can be interpreted as the result of the different displacement of guest atoms in the cage, namely, "rattling" in these samples of type-I clathrates. Consequently, the size difference of electrostatic interaction region indicated by the red curve in Fig. 3(b) visualizes the difference of the guest atom's motion in the cage. In addition, the shape of the interaction region can provide us the characteristics of the guest atom's displacement. For instance, all compounds show the directional deformation of the interaction region toward the next cage. In addition, *p*-BGG exhibits further directional deformation of the interaction region toward the G1 site, suggesting the site-dependent interaction due to the specific atom deficiency of the G1 site. The results show that the electrostatic-potential analysis is a powerful tool to unveil the dynamical phenomena and/or stationary displacement of the guest atoms inside the cage structure; even a subtle feature occurs in the type-I clathrate compounds, $X_8Ga_{16}Ge_{30}$, which was not achieved by the MEM charge-density analysis.

D. Quantitative analysis of effect of rattling

We, then, quantitatively evaluate the order of effect of the rattling with the volume inside the EPLMS (V_{EP}) by comparing it to the spherical volume using the covalent radius[52] of the atom (V_{cov}):

$$f_R = V_{EP}/V_{cov}. \quad (1)$$

The values of f_R are about 0.90, 1.13, and 1.22 for *n*-BGG, *p*-BGG, and *n*-SGG, respectively. This relation can be clearly confirmed by comparing the trace of EPLMS (red curves) and circles with covalent radius (blue curves) in Fig. 3(b): circles with covalent radius for *p*-BGG and *n*-SGG are included in the region surrounded by the EPLMS, whereas the circle for *n*-BGG is not. All parameters are summarized in Table II. The result can be reasonably understood as follows: the guest atom hardly affects the coherent phonon of the cage when the weak interaction region (inside the EPLMS) does not exceed the covalent radius, which corresponds to the short and strong bond, namely, $f_R < 1$. The degree of phonon scattering by the guest atom increases with increasing f_R. It seems to be reasonable that $f_R = 1$ shall allow to define a border between the phonon-glass and conventional phonon states of the type-I clathrates. Actually, total κ for these compounds at 20 K monotonously decreases with an increase of f_R, as shown in Fig. 4. This tendency is enhanced by taking account of the

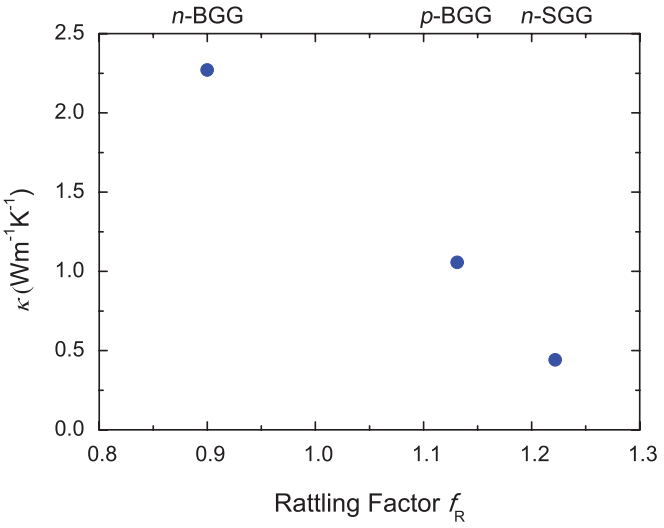

FIG. 4. (Color online) Relation between rattling factor and thermal conductivity. Both values were estimated using data measured at 20 K.

lattice thermal conductivity κ_L.[16,17] It should be noted that our conclusion does not change qualitatively by the use of values normalized by other radii, such as ionic radii, Van der Waals radii, and atomic radii, although the quantitative aspect, for example, a value of border between the phonon-glass and conventional phonon states depends on the kind of referred radius. On the other hand, the ratio of V_{EP} to the cage size V_{cage} is not good parameter for explaining the reduction of κ, because V_{cage} is almost the same for all three compounds, and the absolute value of V_{EP} does not show the monotonous relation to κ. These suggest that the value of f_R can be defined as a measure to characterize the effect of the rattling in the type-I clathrates free from the origins of the rattling, such as the cage defects for *p*-BGG and the ionic size for *n*-SGG. This estimation will be quite effective for materials, which can be provided only in small quantities and can be characterized only by x-ray diffraction analysis.

IV. CONCLUSIONS

We succeeded in parameterization of the effect of the rattling, off-center distribution of the guest atom in the clathrates, relating to the suppression of thermal conductivity based on the electrostatic-potential analysis using MEM electron density. Our finding of the structural criterion, "rattling factor" f_R with the Eq. (1), shall become a powerful tool to discuss the rattling influencing the thermoelectric property of various kinds of clathrates, in spite of statistical analysis using time-integrated structural data. We believe that this method can be extended as a tool for systematic characterization of peculiar chemical and/or physical properties of materials originating from subtle structural differences.

ACKNOWLEDGMENTS

We thank Y. Iwasa and M. Sakata for valuable discussions. The single-crystal synchrotron radiation x-ray diffraction measurements were carried out at BL02B1, SPring-8, Japan (Proposal No. 2009B1144) with support from the Power User program. This work was supported in part by Grant-in-Aid for Scientific Research on Priority Areas: New Materials Science Using Regulated Nano Spaces-Strategy in Ubiquitous Elements (19051004) from the Ministry of Education, Culture, Sports, Science and Technology of Japan and the Tohoku University GCOE program: Particle-Matter Hierarchy of MEXT, Japan.

*fujiwara@spring8.or.jp

[1] G. J. Halder, C. J. Kepert, B. Moubaraki, K. S. Murray, and J. D. Cashion, Science **298**, 1762 (2002).
[2] S. Aoyagi, E. Nishibori, H. Sawa, K. Sugimoto, M. Takata, Y. Miyata, R. Kitaura, H. Shinohara, H. Okada, T. Sakai, Y. Ono, K. Kawachi, K. Yokoo, S. Ono, K. Omote, Y. Kasama, S. Ishikawa, T. Komuro, and H. Tobita, Nat. Chem. **2**, 678 (2010).
[3] Z. Hiroi, J. Yamaura, and K. Hattori, J. Phys. Soc. Jpn. **81**, 011012 (2012).
[4] S. Shimomura, M. Higuchi, R. Matsuda, K. Yoneda, Y. Hijikata, Y. Kubota, Y. Mita, J. Kim, M. Takata, and S. Kitagawa, Nat. Chem. **2**, 633 (2010).
[5] B. C. Sales, C. Mandrus, and R. K. Williams, Science **272**, 1325 (1996).
[6] V. Keppens, D. Mandrus, B. C. Sales, B. C. Chakoumakos, P. Dai, R. Coldea, M. B. Maple, D. A. Gajewski, E. J. Freeman, and S. Bennington, Nature (London) **395**, 876 (1998).
[7] M. M. Koza, M. R. Johnson, R. Viennois, H. Mutka, L. Girard, and D. Ravot, Nat. Mater. **7**, 805 (2008).
[8] J. Yamaura and Z. Hiroi, J. Phys. Soc. Jpn. **80**, 054601 (2011).
[9] G. S. Nolas, J. L. Cohn, G. A. Slack, and S. B. Schujman, Appl. Phys. Lett. **73**, 178 (1998).
[10] J. L. Cohn, G. S. Nolas, V. Fessatidis, T. H. Metcalf, and G. A. Slack, Phys. Rev. Lett. **82**, 779 (1999).
[11] J. Yamaura, S. Yonezawa, Y. Muraoka, and Z. Hiroi, J. Solid State Chem. **179**, 336 (2006).
[12] M. Brühwiler, S. M. Kazakov, J. Karpinski, and B. Batlogg, Phys. Rev. B **73**, 094518 (2006).
[13] G. A. Slack, in *CRC Handbook of Thermoelectrics*, edited by D. M. Rowe (CRC, Boca Raton, FL, 1995), Chap. 34, p. 407.
[14] V. Keppens, B. C. Sales, D. Mandrus, B. C. Chakoumakos, and C. Laermans, Philos. Mag. Lett. **80**, 807 (2000).
[15] G. S. Nolas, T. J. R. Weakley, J. L. Cohn, and R. Sharma, Phys. Rev. B **61**, 3845 (2000).
[16] B. C. Sales, B. C. Chakoumakos, R. Jin, J. R. Thompson, and D. Mandrus, Phys. Rev. B **63**, 245113 (2001).
[17] A. Bentien, M. Christensen, J. D. Bryan, A. Sanchez, S. Paschen, F. Steglich, G. D. Stucky, and B. B. Iversen, Phys. Rev. B **69**, 045107 (2004).
[18] A. Bentien, S. Johnsen, and B. B. Iversen, Phys. Rev. B **73**, 094301 (2006).

[19]K. Umeo, M. A. Avila, T. Sakata, K. Suekuni, and T. Takabatake, J. Phys. Soc. Jpn. **74**, 2145 (2005).
[20]M. A. Avila, K. Suekuni, K. Umeno, and T. Takabatake, Physica B **383**, 124 (2006).
[21]J. Tang, R. Kumashiro, J. Ju, Z. Li, M. A. Avila, K. Suekuni, T. Takabatake, F. Guo, K. Kobayashi, and K. Tanigaki, Chem. Phys. Lett. **472**, 60 (2009).
[22]J. Xu, J. Tang, K. Sato, Y. Tanabe, H. Miyasaka, M. Yamashita, S. Heguri, and K. Tanigaki, Phys. Rev. B **82**, 085206 (2010).
[23]M. Christensen, N. Lock, J. Overgaard, and B. B. Iversen, J. Am. Chem. Soc. **128**, 15657 (2006).
[24]I. Zerec, V. Keppens, M. A. McGuire, D. Mandrus, B. C. Sales, and P. Thalmeier, Phys. Rev. Lett. **92**, 185502 (2004).
[25]M. Christensen, A. B. Abrahamsen, N. B. Christensen, F. Juranyi, N. H. Andersen, K. Lefmann, J. Andreasson, C. R. H. Bahl, and B. B. Iversen, Nat. Mater. **7**, 811 (2008).
[26]Y. Takasu, T. Hasegawa, N. Ogita, M. Udagawa, M. A. Avila, K. Suekuni, I. Ishii, T. Suzuki, and T. Takabatake, Phys. Rev. B **74**, 174303 (2006).
[27]Y. Takasu, T. Hasegawa, N. Ogita, M. Udagawa, M. A. Avila, K. Suekuni, and T. Takabatake, Phys. Rev. Lett. **100**, 165503 (2008).
[28]Y. Takasu, T. Hasegawa, N. Ogita, M. Udagawa, M. A. Avila, K. Suekuni, and T. Takabatake, Phys. Rev. B **82**, 134302 (2010).
[29]T. Mori, S. Goshima, K. Iwamoto, S. Kushibiki, H. Matsumoto, N. Toyota, K. Suekuni, M. A. Avila, T. Takabatake, T. Hasegawa, N. Ogita, and M. Udagawa, Phys. Rev. B **79**, 212301 (2009).
[30]H. Matsumoto, T. Mori, K. Iwamoto, S. Goshima, S. Kushibiki, and N. Toyota, Phys. Rev. B **79**, 214306 (2009).
[31]T. Mori, K. Iwamoto, S. Kushibiki, H. Honda, H. Matsumoto, N. Toyota, M. A. Avila, K. Suekuni, and T. Takabatake, Phys. Rev. Lett. **106**, 015501 (2011).
[32]R. Baumbach, F. Bridges, L. Downward, D. Cao, P. Chesler, and B. Sales, Phys. Rev. B **71**, 024202 (2005).
[33]J. Tang, T. Rachi, R. Kumashiro, M. A. Avila, K. Suekuni, T. Takabatake, F. Z. Guo, K. Kobayashi, K. Akai, and K. Tanigaki, Phys. Rev. B **78**, 085203 (2008).
[34]L. Gil, M. A. Ramos, A. Bringer, and U. Buchenau, Phys. Rev. Lett. **70**, 182 (1993).
[35]M. A. Ramos and U. Buchenau, Phys. Rev. B **55**, 5749 (1997).
[36]J. Dong, O. F. Sankey, and C. W. Myles, Phys. Rev. Lett. **86**, 2361 (2001).
[37]C. Gatti, L. Bertini, N. P. Blake, and B. B. Iversen, Chem. Eur. J. **9**, 4556 (2003).
[38]F. Bridges and L. Downward, Phys. Rev. B **70**, 140201(R) (2004).
[39]B. B. Iversen, A. E. C. Palmqvist, D. E. Cox, G. S. Nolas, G. D. Stucky, N. P. Blake, and H. Metiu, J. Solid State Chem. **149**, 455 (2000).
[40]A. Bentien, A. E. C. Palmqvist, J. D. Bryan, S. Latturner, G. D. Stucky, L. Furenlid, and B. B. Iversen, Angew. Chem. Int. Ed. **39**, 3613 (2000).
[41]D. T. Cromer, J. Appl. Crystallogr. **16**, 437 (1983).
[42]Crystal data for *n*-BGG: $Ba_8Ga_{16}Ge_{30}$, $M_r = 4391.94$, cubic, space group $Pm\bar{3}n$, $a = 10.7314(7)$ Å, $V = 1235.86(14)$ Å^3, $Z = 1$, $T = 20$ K, $\rho_{calcd} = 5.901$ gcm^{-3}, $\mu = 4.552$ mm^{-1}, $d_{max} = 0.46$ Å, 23256 reflections measured ($R_{merge} = 0.0428$), 1206 unique, 796 [$I > 2\sigma(I)$] were used to refine 18 parameters, w$R_2 = 0.0184$, $R_1 = 0.0125$ [$I > 2\sigma(I)$], goodness of fit (GOF) = 0.671. Further details of the crystal structure investigation may be obtained from Fachinformationszentrum Karlsruhe, 76344 Eggenstein-Leopoldshafen, Germany [fax: (+49)7247-808-666; e-mail: crysdata@fiz-karlsruhe.de, http://www.fiz-karlsruhe.de/request_for_deposited_data.html)] on quoting the depository number CSD-422586.
[43]Crystal data for *p*-BGG: $Ba_8(Ga_{16}Ge_{30})_{0.995}$, $M_r = 4375.47$, cubic, space group $Pm\bar{3}n$, $a = 10.7261(2)$ Å, $V = 1234.03(4)$ Å^3, $Z = 1$, $T = 20$ K, $\rho_{calcd} = 5.901$ gcm^{-3}, $\mu = 4.559$ mm^{-1}, $d_{max} = 0.46$ Å, 20781 reflections measured ($R_{merge} = 0.0274$), 1206 unique, 939 [$I > 2\sigma(I)$] were used to refine 22 parameters, w$R_2 = 0.0196$, $R_1 = 0.0104$ [$I > 2\sigma(I)$], GOF = 0.781. Further details of the crystal structure investigation may be obtained from Fachinformationszentrum Karlsruhe on quoting the depository number CSD-422587.
[44]Crystal data for *n*-SGG: $Sr_8Ga_{16}Ge_{30}$, $M_r = 3994.18$, cubic, space group $Pm\bar{3}n$, $a = 10.6739(3)$ Å, $V = 1216.10(6)$ Å^3, $Z = 1$, $T = 20$ K, $\rho_{calcd} = 5.454$ gcm^{-3}, $\mu = 5.071$ mm^{-1}, $d_{max} = 0.46$ Å, 20940 reflections measured ($R_{merge} = 0.0288$), 1206 unique, 900 [$I > 2\sigma(I)$] were used to refine 24 parameters, w$R_2 = 0.0194$, $R_1 = 0.0113$ [$I > 2\sigma(I)$], GOF = 0.720. Further details of the crystal structure investigation may be obtained from Fachinformationszentrum Karlsruhe on quoting the depository number CSD-422585.
[45]M. Takata, B. Umeda, E. Nishibori, M. Sakata, Y. Saito, M. Ohno, and H. Shinohara, Nature (London) **377**, 46 (1996).
[46]M. Takata, Acta Crystallogr. A **64**, 232 (2008).
[47]H. Tanaka, Y. Kuroiwa, and M. Takata, Phys. Rev. B **74**, 172105 (2006).
[48]K. Kato, Y. Moritomo, M. Takata, H. Tanaka, and N. Hamada, Phys. Rev. B **77**, 081101(R) (2008).
[49]M. Takata, E. Nishibori, M. Sakata, M. Inakuma, E. Yamamoto, and H. Shinohara, Phys. Rev. Lett. **83**, 2214 (1999).
[50]Y. Kubota, M. Takata, R. Matsuda, R. Kitaura, S. Kitagawa, K. Kato, M. Sakata, and T. C. Kobayashi, Angew. Chem. Int. Ed. **44**, 920 (2005).
[51]H. Sawa, Y. Wakabayashi, Y. Murata, M. Murata, and K. Komatsu, Angew. Chem. Int. Ed. **44**, 1981 (2005).
[52]B. Cordero, V. Gómez, A. E. Platero-Prats, M. Revés, J. Echeverría, E. Cremades, F. Barragán, and S. Alvarez, Dalton Trans. 2832 (2008).